processes

MDPI

Article

Advanced Maximum Power Control Algorithm Based on a Hydraulic System for Floating Wave Energy Converters

Chan Roh, Yoon-Jin Ha, Seungh-Ho Shin, Kyong-Hwan Kim and Ji-Yong Park *

Research Institute of Ships and Ocean Engineering (KRISO), 1312-32 Yuseong-daero, Yuseong-gu, Daejeon 34103, Korea; rohchan@kriso.re.kr (C.R.); yj_ha0811@kriso.re.kr (Y.-J.H.); shinsh@kriso.re.kr (S.-H.S.); kkim@kriso.re.kr (K.-H.K.)

* Correspondence: jypark@kriso.re.kr

Abstract: An integrated analysis is required to evaluate the performance of control algorithms used in power take-off (PTO) systems for floating wave energy converters (FWECs). However, research on PTO systems based on the existing hydraulic device has mainly focused on the input power generation performance rather than on obtaining maximum power through hydraulic device-based electrical load control. The power generation performance is analyzed based on the control variables of the existing torque control algorithm (TCA); however, the amount of power generation for each control variable changes significantly based on the cycle of wave excitation moments. This paper proposes a control algorithm to obtain the maximum power by modeling a hydraulic-device-based integrated FWEC. It also proposes a TCA that can obtain the maximum power regardless of the period of wave excitation moment. The proposed TCA continuously monitors the power generation output and changes the PTO damping coefficient in the direction in which the power generation output can be increased. The proposed TCA increased the output power generation by up to 18% compared to each PTO damping coefficient of the conventional TCA. Thus, the proposed method results in higher power generation regardless of the wave excitation moment cycle and performs better than the existing torque control algorithm.

Keywords: floating wave energy converter; hydraulic device; torque damping control algorithm; power take-off system; power performance; power take-off force

Citation: Roh, C.; Ha, Y.-J.; Shin, S.-H.; Kim, K.-H.; Park, J.-Y. Advanced Maximum Power Control Algorithm Based on a Hydraulic System for Floating Wave Energy Converters. *Processes* **2021**, *9*, 1712. https://doi.org/10.3390/pr9101712

Academic Editor: Kody Powell

Received: 31 July 2021
Accepted: 19 September 2021
Published: 24 September 2021

1. Introduction

The concept of floating wave energy converters (FWECs) is based on the extraction of wave energy using floating bodies in the sea. There are various types of FWECs [1–3] such as the WaveStar, AquaBuoy, PowerBuoy, Pelamis, etc. In a FWEC, the floating body is moved using wave energy, and the power take-off (PTO) system generates electricity using the motion of the floating body. The major issue with a FWEC is that the movement of the floating body caused by the waves is very slow, and it moves irregularly and in both directions [1–4]. The results obtained from the Wavestar, a representative FWEC, show that a bidirectional load torque of 1 MNm is required to extract an average of 27 kW of electricity [4,5]. A wave energy converter has a factor of 10 or greater between the average and peak power [6]. However, the peak power cannot simply be discarded, as it contributes significantly to the overall production. Consequently, energy storage is required to store the energy peaks and maintain the variability in the wave energy using an electrical energy storage system and supercapacitor [7–9].

In relation to the implementation of the PTO system for a FWEC, a study was conducted on a linear generator that was directly driven by the movement of a floating body. However, owing to the slow speed of movement, the existing permanent magnet linear generator inadvertently becomes very large. A conventional FWEC, such as the Wavestar, requires a load force of 400 kN, and the air gap shear stress level of a conventional linear generator is 20–25 kN/m^2 [10]. In other words, even if the necessary support structure

is ignored, the weight is too large to allow the implementation of a linear generator [11]. Methods that use mechanical transmission (a gearbox, etc.) have also been studied; however, the increase in size owing to the high gearing ratio and the characteristics of the bidirectional motion made implementation difficult.

A hydraulic system is a suitable technology for implementing transmission for a FWEC. It can control a high force at a low speed, while the small actuator (cylinder) can easily control the movement in both directions. However, such systems can fail due to practical problems with the design, manufacture and installation of the hydraulic PTO [12,13]. That is, a hydraulic PTO can increase the complexity of the system.

The earliest hydraulic PTO system for the FWEC is shown in Figure 1a. The cylinder functions as a pump, creating a bidirectional flow that drives the hydraulic motor. The hydraulic motor drives the generator, which rotates in one direction only. However, for the Wavestar FWEC in [14], various processes were applied to optimize the PTO from the wave energy to grid power. At the optimum point, the overall PTO power conversion efficiency was 65%, but it quickly dropped to 45% in small waves. However, the system shown in Figure 1a has disadvantages, including the unavailability of energy storage and smoothing. Therefore, a PTO system with a cylinder actuated by a manual pump for constant pressure, as shown in Figure 1b, was used in [15,16], where energy smoothing was performed using an accumulator. This allows hydraulic motors and generators to operate at fairly constant loads, resulting in PTO efficiencies of up to 80%. However, the cylinder is limited to providing a coulomb-like force load, which reduces the amount of absorbed energy [17,18]. Therefore, the authors of [19,20] proposed a hydraulic transformer that can control the force of the cylinder to overcome the coulomb-like force load. However, the load efficiency of hydraulic transformers is poor because the two variable displacement pumps/motors are in series.

In [21], the discrete control of hydraulic cylinders was applied. Mobile hydraulics were investigated and the results indicated a promising increase in energy efficiency as compared to conventional load-sensing systems. In addition, in [22], a PTO system using two asymmetric cylinders was discussed, and the efficiency of controlling the force of the cylinder using pressure movement was found to be between 88% and 94%, excluding the friction of the cylinder. In [23], a hydraulic transmission with an accumulator for energy smoothing operated at 70% efficiency. Similarly, in [24], a system similar to that in [22] was proposed. Moreover, it was tested as a scale version capable of applying a torque of 16 kNm to the system [24,25]. The overall efficiency was estimated to fall in the range of 69% to 80%.

The maximum output control was analyzed through the electrical load control of the power converter instead of the mechanical control, using the discrete displacement cylinder system [19,26]. In these studies, the hydraulic transmission system described in [17,18] was used. The load control method discussed in [17,18] is difficult to apply directly to an actual system because only the theoretical load control is mentioned. In [27], the power generation performance of a PTO system based on a hydraulic system was analyzed through the load control of the power converter. The power generation performance was analyzed by changing the control variable to adjust the PTO damping coefficient. However, it was difficult to select the optimal PTO damping coefficient under irregular input conditions; thus, a PTO damping coefficient that could increase output by changing several control variables was selected. However, the amount of power generation varied greatly depending on the wave excitation moment.

Therefore, this paper proposes a torque control algorithm (TCA) that continuously monitors the output generation and changes the PTO damping coefficient in a direction that increases the output generation. The proposed TCA compared the power generation performance with the conventional TCA, under the same input conditions, using an integrated performance model of the FWEC. Because the power generation output of the conventional TCA changes according to the change in the control variable, the performance of the proposed algorithm was compared based on various control variables.

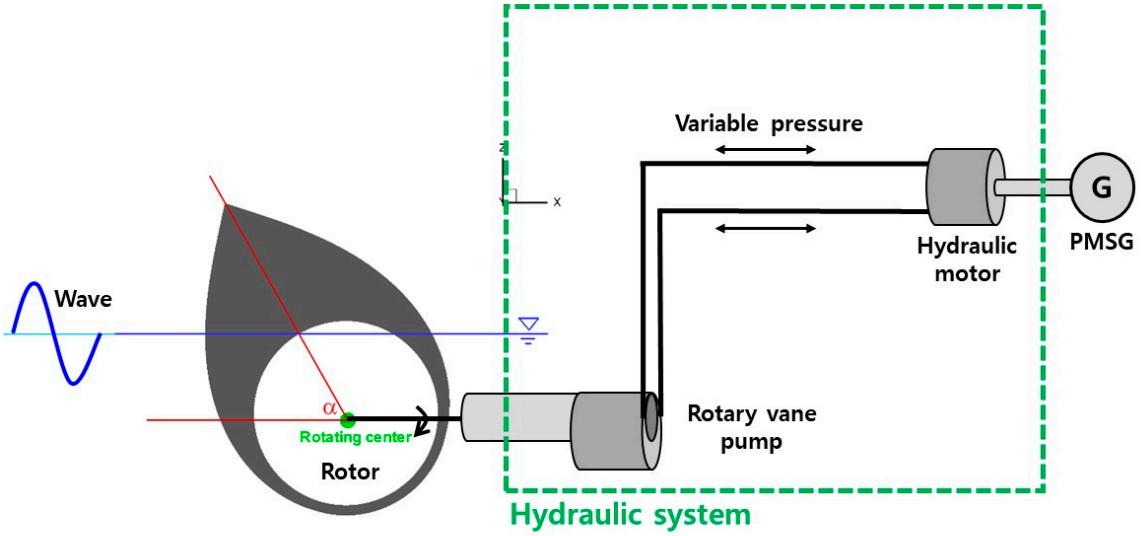

(**a**)

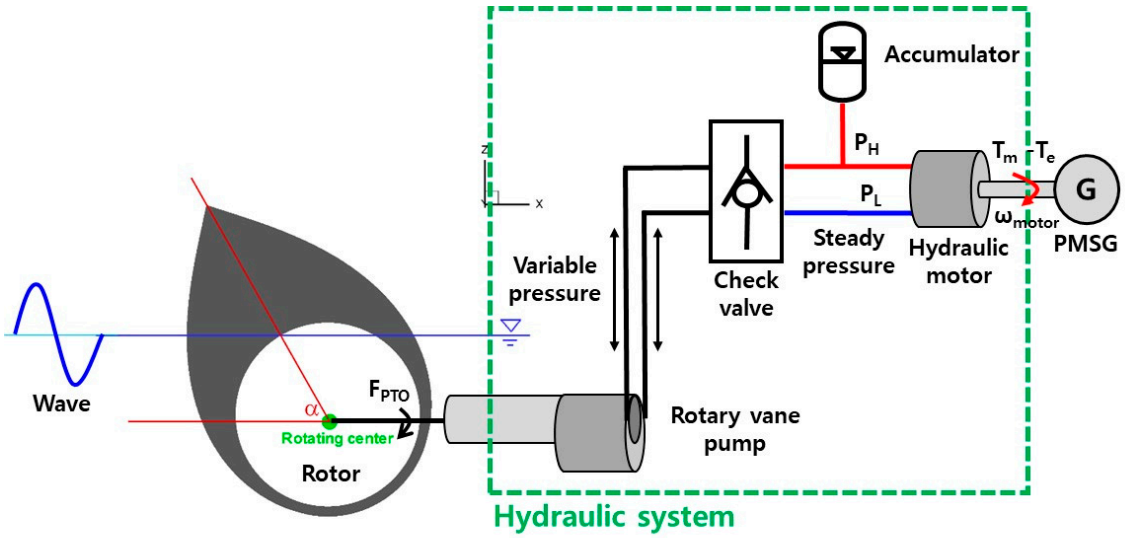

(**b**)

Figure 1. Hydraulic transmission system basic model configuration: (**a**) direct hydraulic motor system, (**b**) hydraulic motor system with an accumulator.

2. Modeling of the Energy Conversion System and Existing Control Techniques for FWECs

2.1. Composition and Classification of Energy Conversion System

A FWEC converts wave energy into relative linear motion or relative rotational motion. In addition, the energy converter converts mechanical power into electrical power. The energy conversion structure used in this study is shown in Figure 2. According to the wave energy converter database of the Office of Energy Efficiency and Renewable Energy (EERE), there are 34 energy conversion structures with technology readiness level (TRL) 5 or higher. Among them, the most commonly used PTO system is the hydraulic system [27,28]. The wave excitation moment variability is substantial owing to the characteristics of the FWEC, which suggests the need for the development of an efficient and reliable PTO system for

energy converters. Therefore, because the hydraulic system of the FWEC is suitable for stable power generation, it was used as the PTO system in this study.

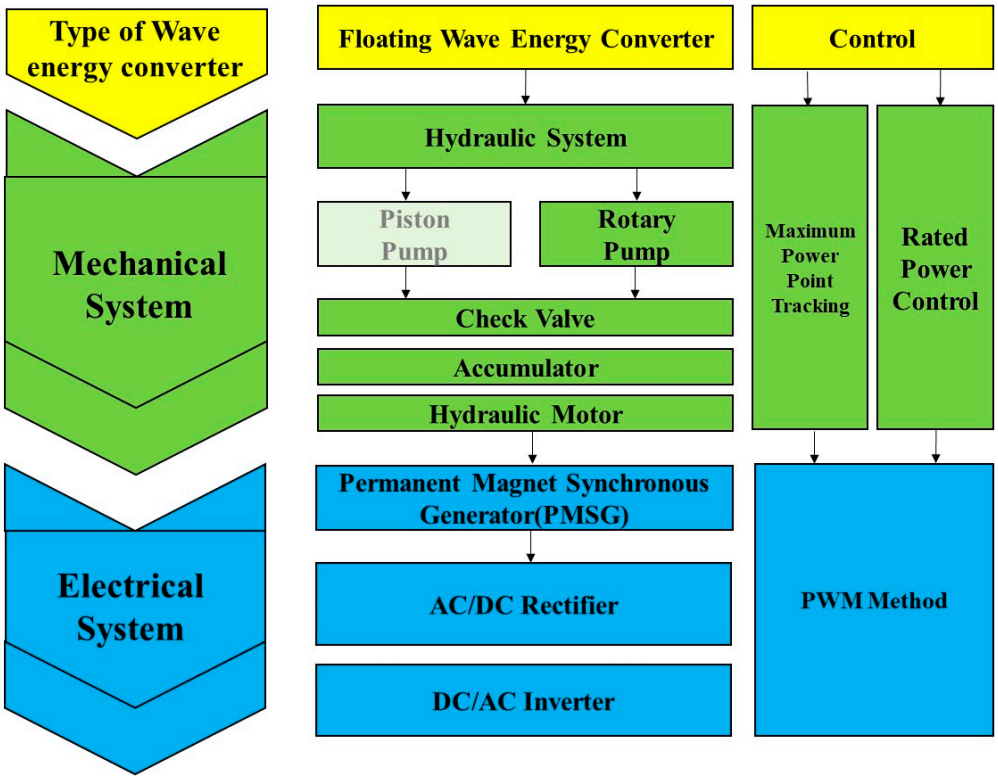

Figure 2. Configuration diagram and control method of the energy conversion system of a floating wave energy converter (FWEC).

The following studies were conducted on the control method of FWECs. The main purpose of such control methods in an FWEC is to generate an optimal PTO force set value [29]. In the early days of control studies, in order to avoid the difficulties of implementing feedback control, the passive load of the linear damping of the PTO [30] or resistive loading was used [31]. The authors of [32] analyzed the kinetic effect of FWEC according to the force of the PTO; that is, the effect of the PTO damping factor on power absorption was analyzed. Another study on real-time PTO attenuation control increased the output efficiency from 21% to 65% by varying the PTO attenuation coefficient to the wave excitation moment [33]. Among these real-time controls, in [34] a non-linear control was implemented by configuring the control considering both the resistive and reactance components of the PTO force. The authors of [35] applied latching control to achieve resonance of FWEC, thus increasing the efficiency of the device. However, when there was no device speed, an external energy source was required. Wu et al. [36] quantified the results of latching control. Furthermore, more recently, model predictive control was applied due to its ability to process linear and non-linear models [37]. However, further research is still needed depending on the optimization problem. In conclusion, studies on various control strategies to adjust the PTO damping coefficient for the FWEC control method have been conducted. However, there is a lack of research on applying the control method to the actual PTO system (hydraulic system, generator, power converter). In this study, a control technique applied to a practical PTO system is presented.

The configuration of the FWEC was as follows. The float used a Salter's duck and converted wave energy into pitch motion. The pitch motion of the floating body was converted into bidirectional rotational motion using a rotary vane pump. As shown in Figure 2, a study using a conventional piston pump was conducted, but the piston pump had a relatively low efficiency as compared to the rotary vane pump. The bidirectional

flow generated by the rotary vane pump was converted into a unidirectional flow through the check valve. The flow from the check valve flows to the accumulator and hydraulic motor, and the flow to the hydraulic motor and the accumulator were determined using the electrical torque. The rotational speed of the generator was determined based on the flow rate of the hydraulic motor. However, the current of the power converter was controlled to control the load and obtain the maximum power with respect to the rotational speed. In other words, it is possible to obtain the maximum amount of power generation through appropriate load current control, based on the wave excitation moment.

Furthermore, the control method of the FWEC was divided into parts for the mechanical and electrical systems, as shown in Figure 2. The mechanical system control was divided into a maximum power point tracking (MPPT) control to absorb the maximum power, and rating control for the protection of the mechanical system. Additionally, the control for the electrical system uses the PWM control method to control the implementation of the MPPT control and rating control. In this paper, we conducted a study on an MPPT control that can obtain maximum power, and the specific load control algorithm is described in detail in the next section.

2.2. Energy Conversion System Modeling

A hydraulic system was used as a suitable PTO system for the FWEC because it provides low speed and high torque. In particular, it can generate stable power using an accumulator, even with irregular wave energy. Figure 3 summarizes the FWEC energy conversion system modeling.

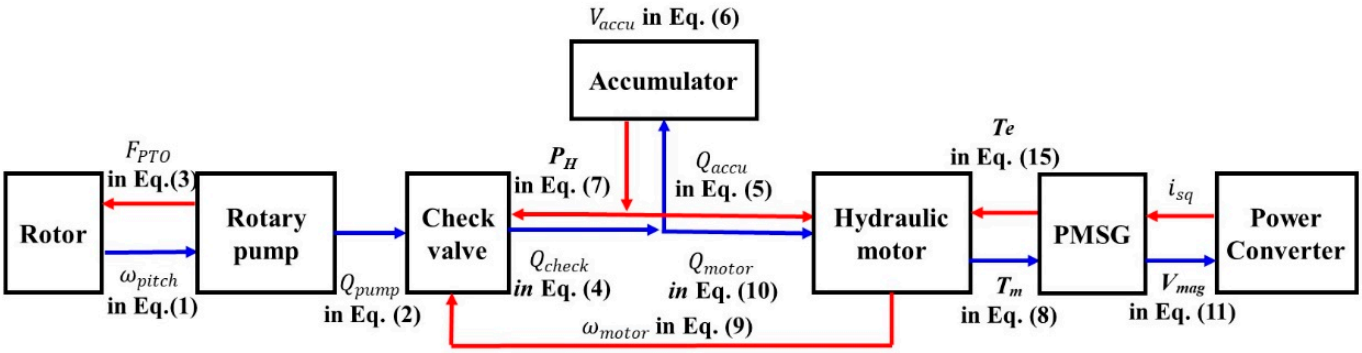

Figure 3. Energy conversion system modeling composition for a FWEC.

The flow rate generated by the rotary vane pump using the pitch angle of the floating body, θ_{pitch} can be expressed as follows:

$$\omega_{pitch} = \frac{d}{dt}\theta_{pitch} \tag{1}$$

$$Q_{pump} = D_{pump} * \omega_{pitch} \tag{2}$$

The pitch angle of the floating body moves according to the wave excitation moment, but is also affected by the PTO force generated by the hydraulic system, which is given by

$$F_{PTO} = D_{pump} * (P_H - P_L) * sign(\omega_{pitch}) \tag{3}$$

The flow generated by the rotary vane pump is bidirectional and can be converted into a unidirectional flow through a check valve, as follows:

$$Q_{check} = |Q_{pump}| \tag{4}$$

The flow rate of the check valve is the sum of the flow rates of the accumulator and hydraulic motor.

$$Q_{check} = Q_{accu} + Q_{motor} \tag{5}$$

The hydraulic system circuit pressure can be calculated based on the accumulator flow rate, which in turn impacts the change in the accumulator volume. The pressure increases based on the chain reactions. The change in pressure based on the accumulator flow rate can be calculated as follows:

$$V_{accu} = \int Q_{accu} dt \tag{6}$$

$$P_H = \frac{P_{H\_pre}}{(V_{accu}/V_{accu\_pre})^{\gamma}} \tag{7}$$

Because the accumulator pressure is equal to the pressure in the circuit, the pressure of the hydraulic motor can also be calculated based on the pressure of the accumulator. Therefore, the mechanical torque of the hydraulic motor is calculated as follows:

$$T_m = D_{motor} * (P_H - P_L) \tag{8}$$

The dynamic state of the hydraulic motor was modeled using the mechanical torque of the hydraulic motor, electrical torque of the generator, and mechanical friction:

$$\frac{d}{dt}\omega_{motor} = 1/J(T_m - T_e - T_{fric}) \tag{9}$$

The rotational speed of the hydraulic motor was impacted by the electrical torque; hence the flow rate of the hydraulic motor can be calculated using rpm as follows:

$$Q_{motor} = D_{motor} * \omega_{motor} \tag{10}$$

That is, the rotational speed and flow rate of the hydraulic motor change according to the electrical load, and the flow rate of the accumulator changes according to Equation (5), thereby changing the pressure in the circuit. In turn, the pressure in the circuit affects the movement of the floating body, according to Equation (3), which affects the overall amount of power generation.

Because the PMSG is directly connected to the hydraulic motor, the mechanical dynamic state of PMSG can be expressed using Equation (9); that is, the magnitude of the output voltage of the generator based on the angular velocity of the PMSG can be calculated as follows:

$$V_{mag} = k_e * \omega_{motor} \tag{11}$$

In addition, in the case of a three-phase balanced system, the instantaneous power (Pe) output by the PMSG can be expressed as

$$P_e = \frac{3}{2}(V_{sd}i_{sd} + V_{sq}i_{sq}) \tag{12}$$

If the loss due to the resistance is miniscule, the P_e of the generator can be expressed as

$$P_e = \frac{3}{2}\left[\omega_e \Psi_{pm} i_{sq} - \omega_e (L_{sd} - L_{sq}) i_{sd} i_{sq}\right] \tag{13}$$

Because the permanent magnet synchronous generator considered in this paper uses the rotor-type structure, L_{sd} and L_{sq} are the same; hence, Equation (13) can be rearranged as follows:

$$P_e = \frac{3}{2}\omega_e \Psi_{pm} i_{sq} \tag{14}$$

Using the relationship between the power and torque, the electrical torque (Te) can be calculated as:

$$T_e = \frac{P_e}{\omega_m} = \frac{3}{2}\frac{\omega_e \Psi_{pm} i_{sq}}{\omega_m} = \frac{3}{2} N_p \Psi_{pm} i_{sq} \quad (15)$$

The electrical angular frequency (ω_e) is equal to the number of dipoles of the rotor (N_p) and the angular velocity of the hydraulic motor (ω_m). From Equation (15), it can be observed that the electrical torque is proportional to the stator q-axis current. The stator q-axis current for the electrical torque can be controlled through the current controller of the power converter.

2.3. Conventional Maximum Power Control for Floating Wave Energy Converter

According to the characteristics of the FWEC, it is necessary to absorb a large amount of wave excitation moment to increase the amount of power generation. This is because the efficiency of the energy conversion system is relatively high. The absorbed power of a FWEC can be calculated using the motion of the floating body and the force of the PTO. There is a portion that becomes the maximum power point for the absorbed power as the motion of the floating body changes according to the force of the PTO. The PTO force of the hydraulic transmission system is proportional to the pressure in the circuit, and it can be calculated using Equation (3).

A TCA was applied to the load control algorithm for maximum power control of a FWEC. Torque control can yield the maximum power using the PTO force to satisfy the FWEC resonance condition [22]. To obtain the maximum power, the wave must have a resonance frequency, in which case the wave frequency can be expressed as:

$$\omega_{wave} = \omega_{reson} = \sqrt{A\rho g / (M + \mu(\omega))}. \quad (16)$$

When the wave frequency satisfies Equation (16), the power absorbed by the floating body can be summarized as

$$P_{abs} = \frac{1}{2} B_{pto} |F_{exc}|^2 / \left\{ B_{rad}(\omega) + B_{vis} + B_{pto} \right\}^2. \quad (17)$$

For the absorbed power to be the maximum power, the following equation must be satisfied:

$$\frac{d}{dt} P_{abs} = \frac{1}{2} |F_{exc}|^2 \frac{B_{rad}(\omega) + B_{vis} - B_{pto}}{\left\{ B_{rad}(\omega) + B_{vis} + B_{pto} \right\}^3} \quad (18)$$

$$\frac{d}{dt} P_{abs} = 0. \quad (19)$$

Using Equations (18) and (19), the PTO damping factor for the maximum power can be summarized as:

$$B_{pto}(\omega) = B_{rad}(\omega) + B_{vis}. \quad (20)$$

The optimal PTO damping coefficient in the resonance period can be expressed, but the PTO damping coefficient changes for every period as shown in Figure 4. Figure 4a shows the optimal PTO damping coefficient for each period. Figure 4b presents the output power generation performance obtained using the optimal PTO damping coefficient for each period and the PTO damping coefficient of the resonance period. Because the input wave energy is an irregular input condition, changing the PTO damping coefficient according to the input wave energy period is not feasible. Therefore, the conventional TCA controls the load by using the optimum PTO damping coefficient in the resonance period.

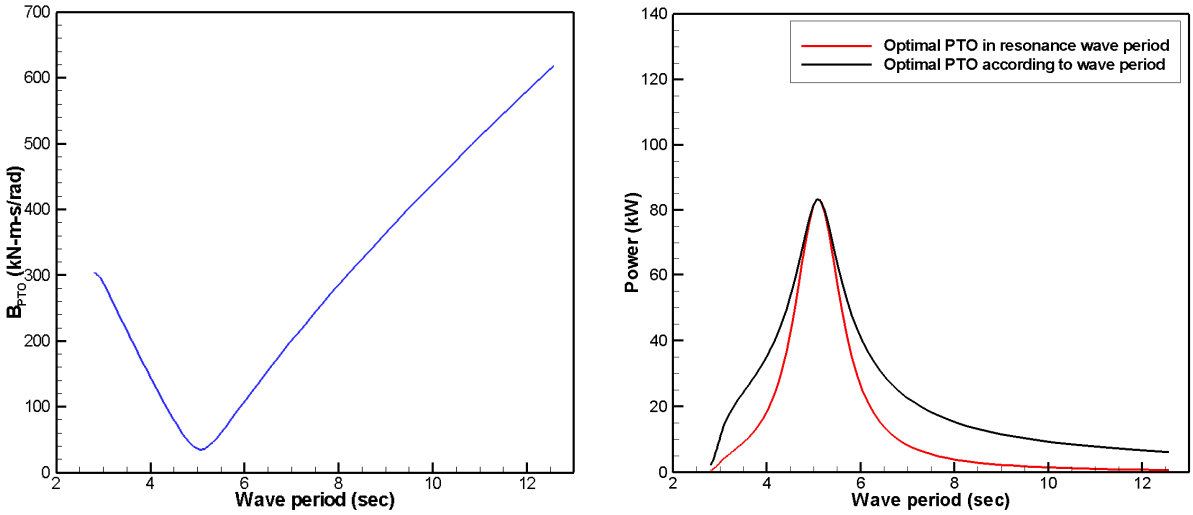

(**a**) (**b**)

Figure 4. (**a**) Optimal PTO damping coefficient for each period, (**b**) Output generation performance according to the optimal PTO damping coefficient for each period and PTO damping coefficient for the resonance period.

If the loss of the PTO system is not considered, the mechanical power can be expressed as the movement of the floating body and the PTO force:

$$P_m = F_{PTO} * \omega_{pitch}. \tag{21}$$

The PTO force can be written as follows, if expressed as a simplified model using the PTO damping coefficient:

$$F_{PTO} = B_{PTO} * \omega_{pitch}. \tag{22}$$

As shown in Equation (21), if the mechanical power is expressed using the optimal PTO damping coefficient calculated to obtain the maximum power, it can be written as:

$$P_{m\_opt} = B_{PTO\_opt} * (\omega_{pitch})^2. \tag{23}$$

If the above equation is expressed using the rotary vane pump volume, hydraulic motor volume, and rpm of the hydraulic motor, it can be written as

$$P_{m\_opt} = B_{PTO\_opt} * \left(\frac{D_{motor}}{D_{pump}}\right)^2 {\omega_{motor}}^2. \tag{24}$$

Using the relationship between the torque and power, the optimum mechanical torque can be calculated as follows:

$$T_{m\_opt} = \frac{T_{m\_opt}}{\omega_{motor}} = B_{PTO\_opt} * \left(\frac{D_{motor}}{D_{pump}}\right)^2 \omega_{motor} \tag{25}$$

$$k_{opt} = B_{PTO\_opt} * \left(\frac{D_{motor}}{D_{pump}}\right)^2. \tag{26}$$

The electrical torque reference value for obtaining the maximum output can be calculated as

$$T_e^* = T_{m\_opt} = k_{opt} * \omega_{motor}. \tag{27}$$

However, under irregular wave input conditions, the optimal PTO damping coefficient may include components of various periods, rather than the resonance period. Therefore, because the conventional TCA applies the damping coefficient value in the resonance

period, the amount of output generation is less than that of the control considering all periods, as shown in Figure 4b. Consequently, in this paper, we conducted a study on a TCA that can overcome this problem.

3. Proposed Control Method for Floating Wave Energy Converter

In the conventional TCA, the maximum power control can be obtained only when the PTO damping coefficient is appropriately selected according to the cycle of the wave excitation moment. However, because the wave excitation moment has irregular characteristics, it includes components of various periods. It is difficult to change the PTO damping coefficient according to the period of the wave excitation moment, hence the conventional TCA is a limited in regard to obtaining the maximum output power.

Therefore, this paper proposes a TCA that can follow the maximum output power according to the change in the input wave energy period. It is impossible to apply the PTO damping coefficient by measuring the period of wave excitation moment, which is why we chose to change the PTO damping coefficient based on monitoring the output power generation. That is, the maximum output power can be obtained by changing the PTO damping coefficient such that the output energy can be increased. Unlike the conventional TCA, which applies a single PTO damping coefficient, the PTO damping coefficient can be changed to continuously monitor the output power generation in order to increase its volume. Figure 5 shows a flowchart of the proposed TCA.

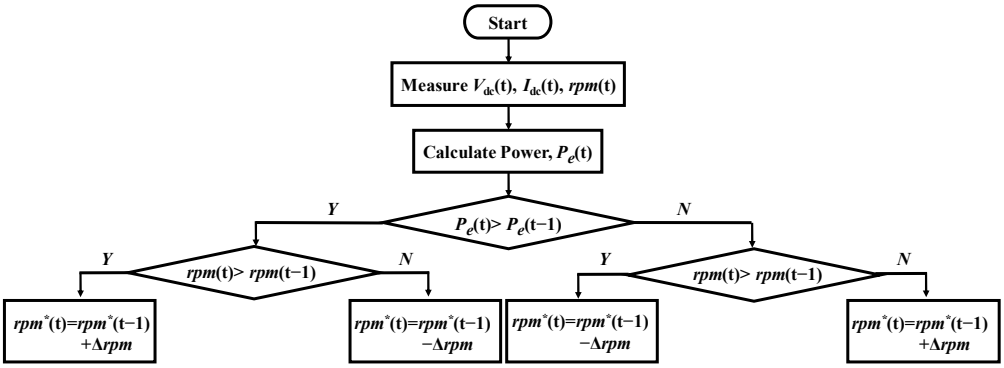

Figure 5. Flowchart of the proposed TCA.

Figure 6 shows the power absorbed by the FWEC based on the PTO force. There is an optimal point at which the absorbed power is maximized. In other words, to obtain the maximum power, the PTO force that is proportional to the circuit pressure of the energy converter must be controlled. The circuit pressure changes according to the PTO damping coefficient of the TCA. That is, the conventional TCA cannot converge to an optimal point if an appropriate PTO damping coefficient is not applied. Therefore, the proposed TCA changes the PTO damping coefficient using the average output amount of the output energy for a certain time, to follow the optimal point based on the wave excitation moment. In the proposed algorithm, when the PTO damping coefficient increases, the pressure in the circuit increases, and the PTO force increases. Similarly, when the PTO damping coefficient decreases, the pressure in the circuit and the PTO force also decreases. Based on this principle, as shown in Figure 6, if the average output for a certain period of time increased from the previous average output, the PTO attenuation coefficient was changed in the existing direction to converge to the optimal value. Conversely, if the average output for a certain period of time decreased as compared to the previous average output, the PTO attenuation coefficient was changed in the opposite direction to the existing trend to converge to the optimal value. Unlike the conventional TCA, it follows the optimal point by changing the PTO damping coefficient according to the wave excitation moment cycle.

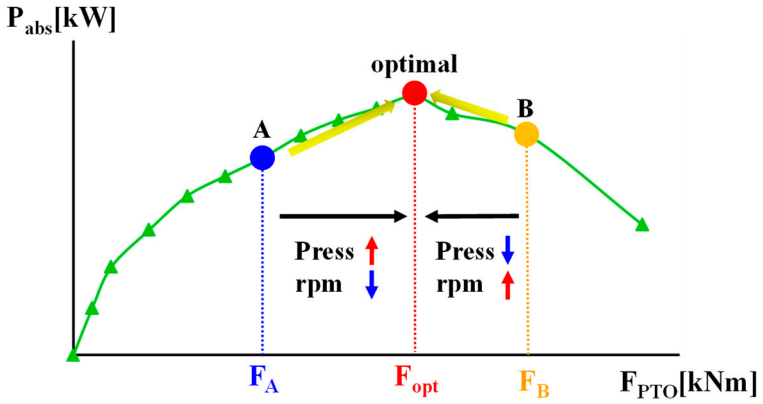

Figure 6. Power generation output characteristics according to PTO.

4. Results

The conventional TCA and the proposed TCA were compared through hydraulic-system-based PTO system modeling. The movement of the floating body in the same wave conditions changed in response to the PTO system characteristics based on the MPPT algorithm, and the overall power generation performance changed accordingly. Through computational fluid dynamics (CFD) analysis, we applied the motion of the floater under the electric load control, as shown in Figure 7a.

Simulations were performed under regular wave conditions, and the power generation performance was compared based on the change in the MPPT algorithm for each set of wave conditions. Figure 8b shows a block diagram of the simulation.

The input condition of the regular wave simulation was compared with the output performance when the period was changed while the wave height was 0.75 m. In the input condition, the pitch angle and absorption power of the floating body based on the load change for each period were calculated using CFD under the 0.75 m wave height condition, as shown in Figure 8 [38].

Figure 8 shows the change in the pitch angle of the floating body and the amount of absorbed power based on the PTO force acting on the floating body. A load that yielded the optimal power generation also occurred as the PTO force increased and the float motion decreased.

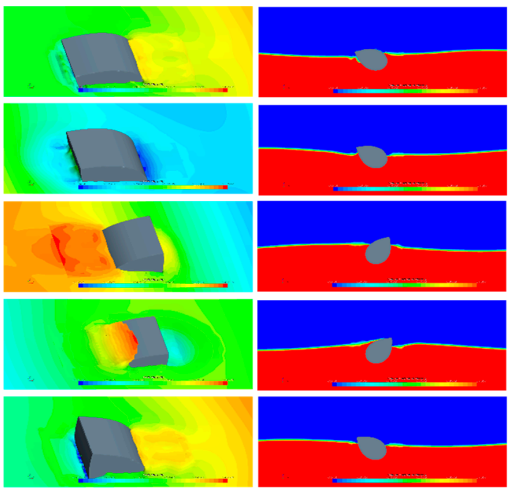

(**a**)

Figure 7. *Cont.*

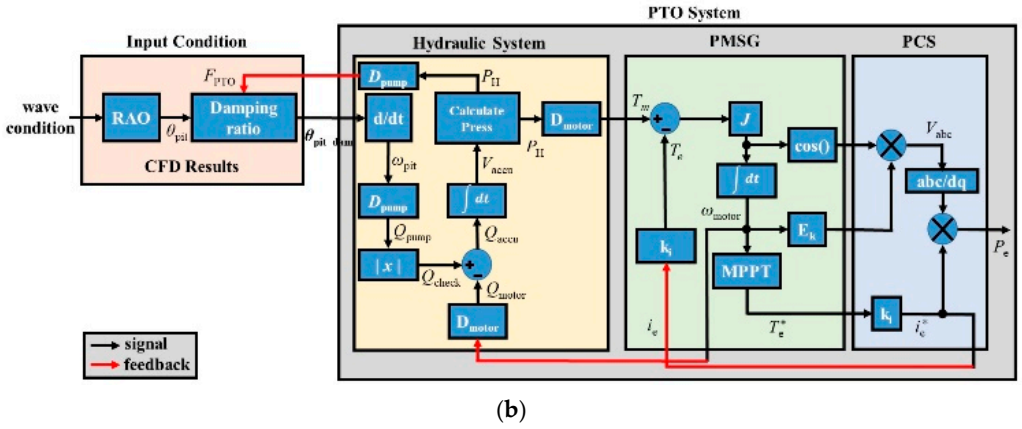

(**b**)

Figure 7. (**a**) CFD analysis plot for input conditions. (**b**) Simulation block diagram for comparison of load control algorithm performance.

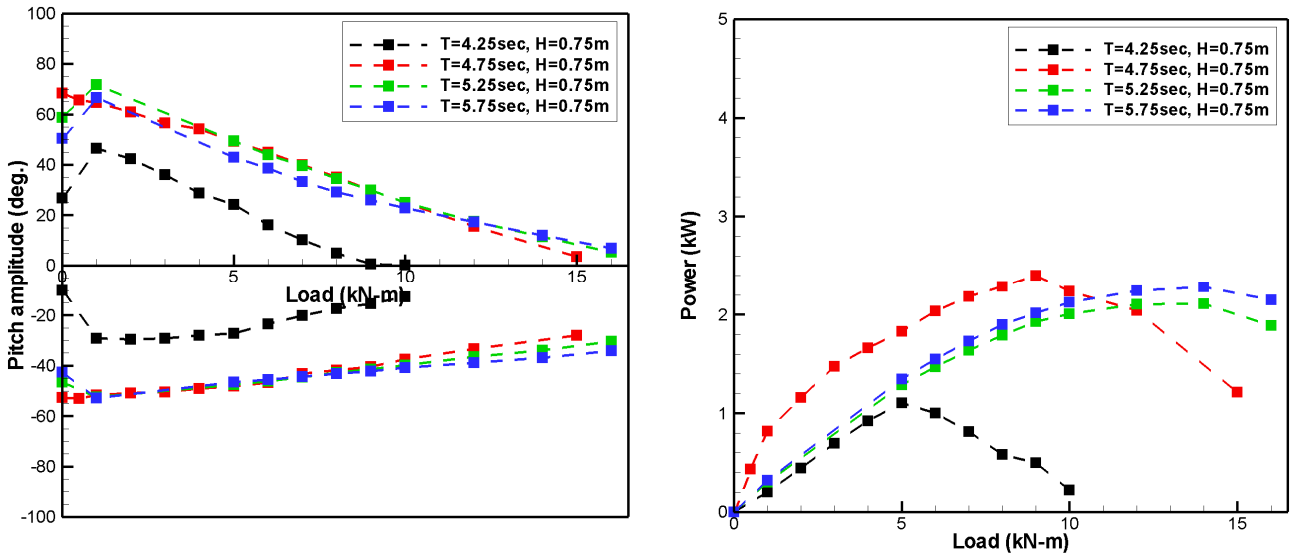

(**a**) (**b**)

Figure 8. (**a**) Pitch angle and (**b**) absorbed power according to PTO force under regular wave conditions with various wave periods.

The power generation performance was compared by applying the proposed TCA and the conventional TCA for maximum power control under the input conditions given below. Based on this, a maximum power control algorithm that is suitable for a hydraulic system-based PTO system was derived. The simulation execution time was 1000 s so that the regular wave characteristics could be understood.

Figure 9 shows the motion of the floating body based on the circuit pressure of the hydraulic system as a result of applying each algorithm, and the PTO force acting on the floating body. The PTO damping coefficient of the conventional TCA was compared by applying a damping coefficient (k_{opt} = 1.5). The conventional TCA had a higher PTO force value because the pressure in the circuit was higher than that of the proposed TCA; consequently, it can be observed that the motion of the floating body was slightly reduced. This confirmed that the pressure in the circuit changes based on the PTO damping coefficient, and subsequently, the motion of the floating body and the PTO force also changes. In conclusion, an optimal PTO damping coefficient is required to control the motion of the floating body to obtain the maximum output. The proposed TCA changes the PTO damping coefficient to increase the power generation output. As shown in Figure 9,

the PTO force value is low because it converges to a lower torque coefficient than the conventional TCA.

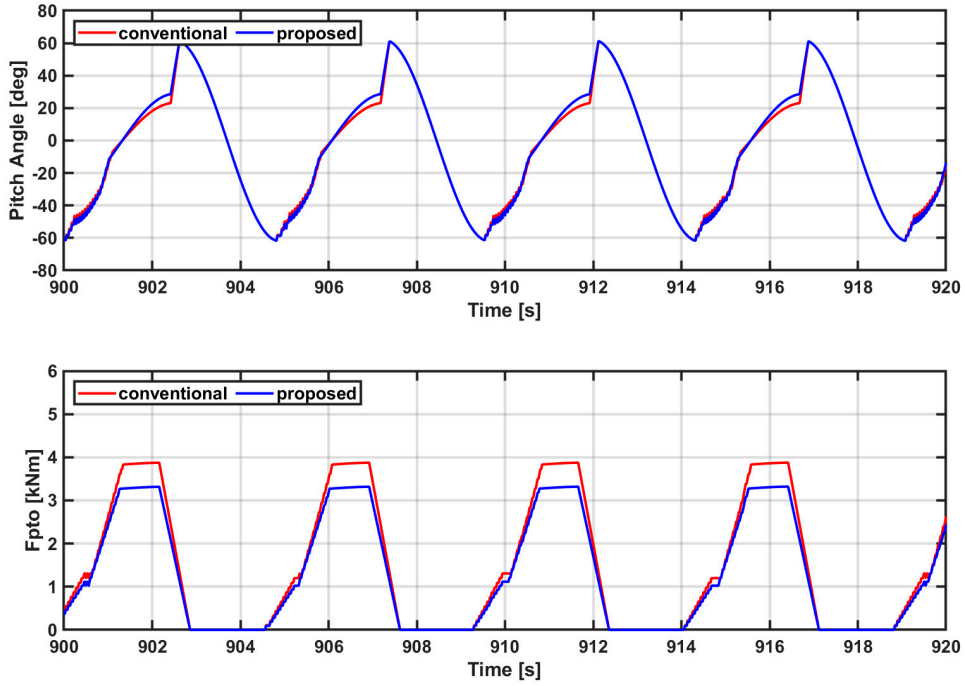

Figure 9. Floating body motion and PTO force based on the conventional TCA and the proposed TCA (H = 0.75 m, T = 4.75 s).

Figure 10 shows the characteristics of the hydraulic system based on the movement of the floating body. These characteristics indicate the pressure in the circuit, the flow rate of the hydraulic motor, and the mechanical and electrical torque. In the conventional TCA, the flow rate to the hydraulic motor was reduced because the pressure in the circuit was high. It can be observed that more flow was introduced into the accumulator to increase the pressure in the circuit. Consequently, it was confirmed that the torque of the hydraulic motor is also high in conventional TCA. Because the proposed TCA continuously changes the PTO damping coefficient in terms of output power generation, it converges to a lower PTO damping coefficient than the conventional TCA. Thereby, it was confirmed that the proposed TCA has low pressure in the circuit and a low torque of the hydraulic motor.

Figure 11 shows the power generation for each algorithm, which was compared using a power generator. Unlike the conventional TCA, the proposed TCA continuously monitors the output power to change the PTO damping coefficient, such that it can obtain higher power generation than a single PTO damping coefficient. Thus, if a fixed PTO damping coefficient is used, the power generation changes based on the period of the wave excitation moment, and the variations in the power generated are very large.

Figure 12 shows the motion of the floating body based on the circuit pressure of the hydraulic system, and the PTO force acting on the floating body when the wave excitation moment period is increased. A comparison was performed by applying the same PTO damping coefficient (k_{opt} = 1.5) as shown in Figure 9 for the conventional TCA. The conventional TCA has a higher PTO force value because the pressure in the circuit is higher than that in the proposed TCA. Subsequently, it can be observed that the motion of the floating body is slightly reduced. However, the proposed TCA adjusts the PTO force to produce the maximum output by changing the PTO damping coefficient according to the period of wave excitation moment.

Figure 13 shows the characteristics of the hydraulic system for each algorithm. The characteristics of the hydraulic system include the pressure in the circuit, flow rate of the hydraulic motor, and the mechanical and electrical torque. As discussed above, in the

conventional TCA, the pressure in the circuit became high, and the PTO force increased accordingly. Additionally, the rotational speed of the hydraulic motor decreased as the pressure increased. However, the proposed TCA increased the rotational speed of the hydraulic motor by lowering the pressure in the circuit, as compared to the conventional TCA. In conclusion, the proposed TCA is a more efficient method to absorb the maximum power changes in the PTO damping coefficient to obtain higher power.

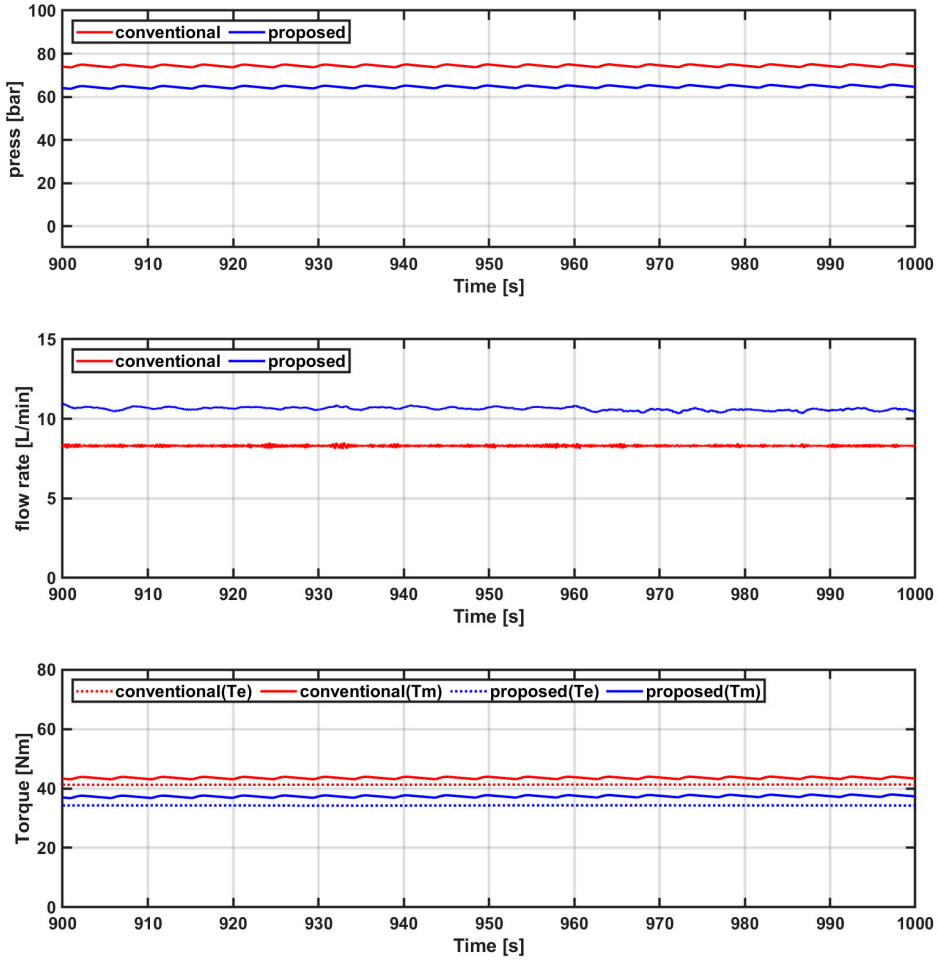

Figure 10. Hydraulic system characteristics according to the conventional TCA and the proposed TCA (H = 0.75 m, T = 4.75 s).

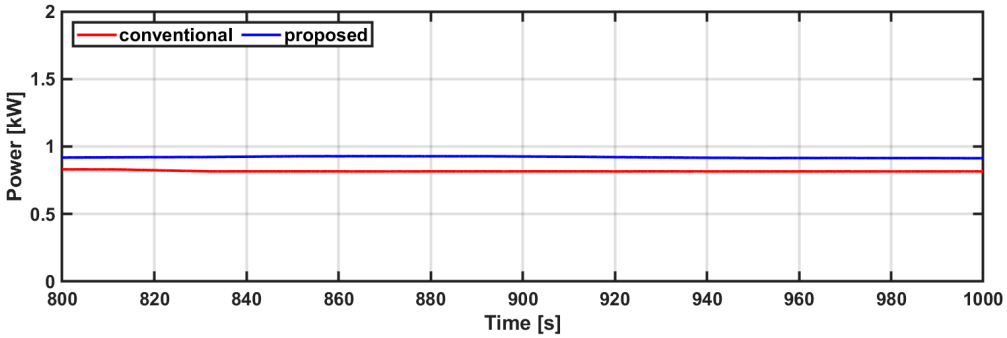

Figure 11. Power generation according to the conventional TCA and the proposed TCA (H = 0.75 m, T = 4.75 s).

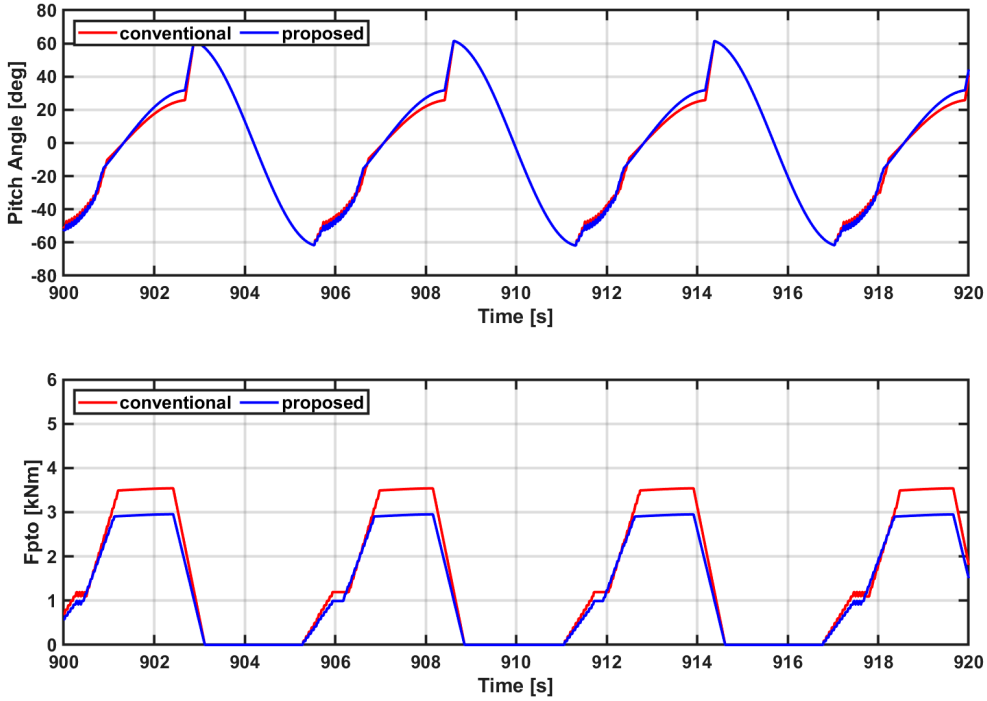

Figure 12. Floating body motion and PTO force based on the conventional TCA and the proposed TCA (H = 0.75 m, T = 5.75 s).

Figure 14 shows the power generation characteristics of each algorithm. Their respective power generation was compared through generator power generation, as shown in Figure 11. Although the period of wave excitation moment was changed, the proposed TCA continuously monitored the output power and changed the PTO damping coefficient. That is, when a fixed PTO damping coefficient was used, as in the case of conventional TCA, the output power changed slightly according to the period of wave excitation moment, and the output power was greatly reduced, as compared to the proposed TCA.

Figure 15 shows the power generation characteristics for each algorithm based on the change in the wave excitation moment period. Because the conventional TCA uses a fixed PTO damping coefficient regardless of the change in the wave excitation moment period, maximum power can only be obtained by determining the optimal PTO damping coefficient, but it may not be possible to do so for each period under irregular input conditions. However, because the proposed TCA changes the PTO damping coefficient in the direction that facilitates an increase in power generation by monitoring, it always obtained a higher power generation output than the conventional algorithm. In conclusion, as shown in Figure 15, the proposed method was able to obtain higher power generation than the conventional TCA in all wave excitation moment periods.

Figure 16 shows the change in the PTO damping coefficient of the conventional algorithm, and the power generation of the proposed algorithm based on the change in the wave excitation moment period. The power generation for each PTO damping coefficient of the conventional TCA, and the power generation of the proposed TCA, were compared according to the change in the wave excitation moment period. The PTO damping coefficients of the conventional TCA were 0.5, 1, 1.5, and 2, respectively. This was compared to the PTO damping coefficients of the proposed TCA. In the conventional TCA, it was confirmed that the PTO damping coefficient that obtains the maximum power generation varies according to the wave excitation moment period. However, because the conventional TCA applies a fixed PTO damping coefficient, the power generation significantly changes based on the wave excitation moment period. Conversely, the proposed method continuously monitors the power generation, and changes the PTO damping coefficient in the direction of increasing power generation; thus, it was confirmed that a high level

of power was always generated, regardless of the wave excitation moment period. In conclusion, as summarized in Figure 16 a comparison of the mean output power of each PTO damping coefficient of the conventional TCA with the mean output power of the proposed TCA in various wave excitation moment periods, shows that the proposed TCA has the largest and an 18% higher power generation output.

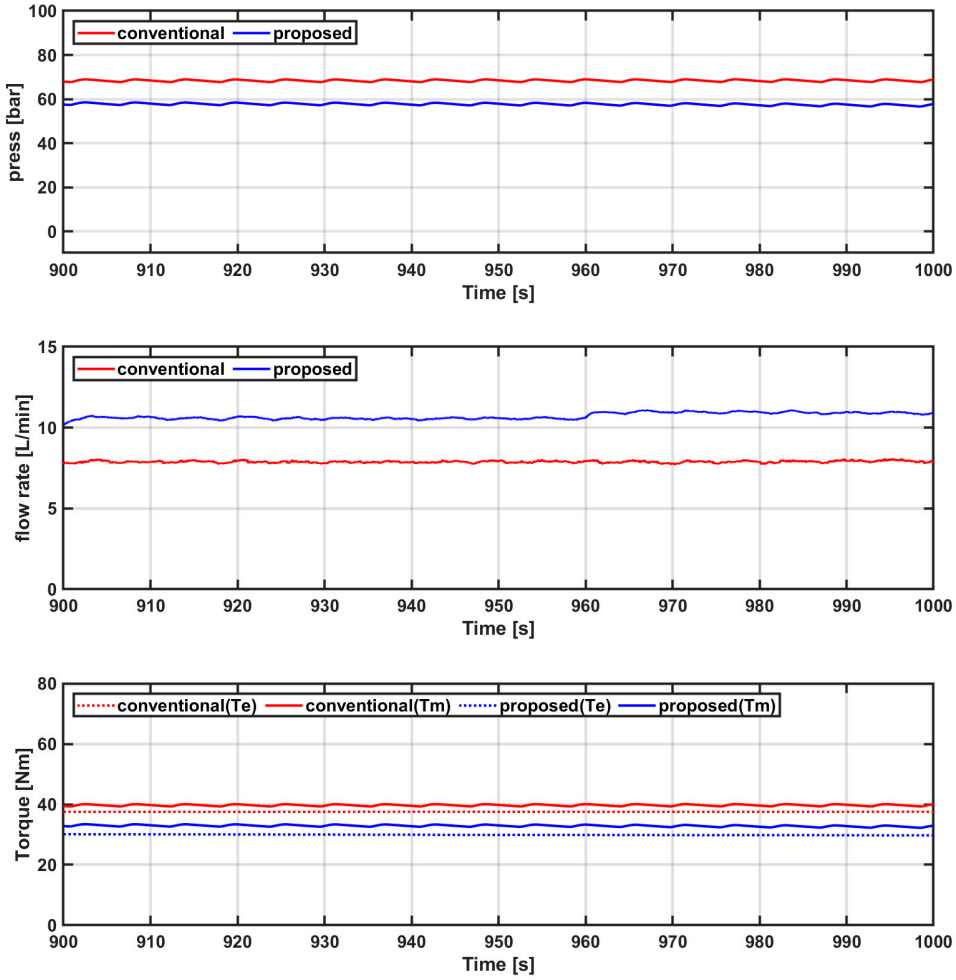

Figure 13. Hydraulic system characteristics according to the conventional TCA and the proposed TCA (H = 0.75 m, T = 5.75 s).

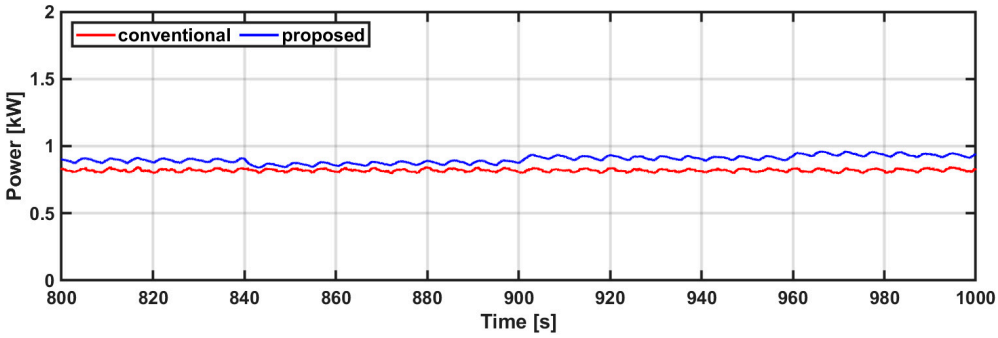

Figure 14. Power generation according to the conventional TCA and the proposed TCA (H = 0.75 m, T = 5.75 s).

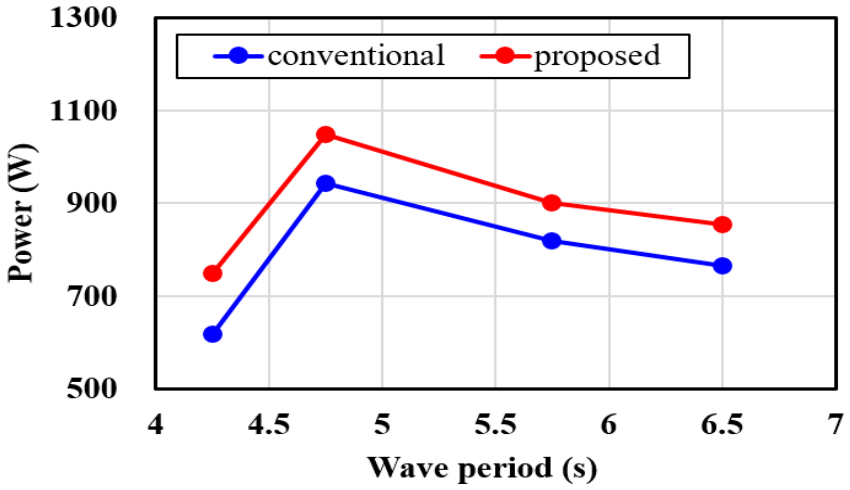

Figure 15. Comparison of power generation of each algorithm according to change in the wave excitation moment period.

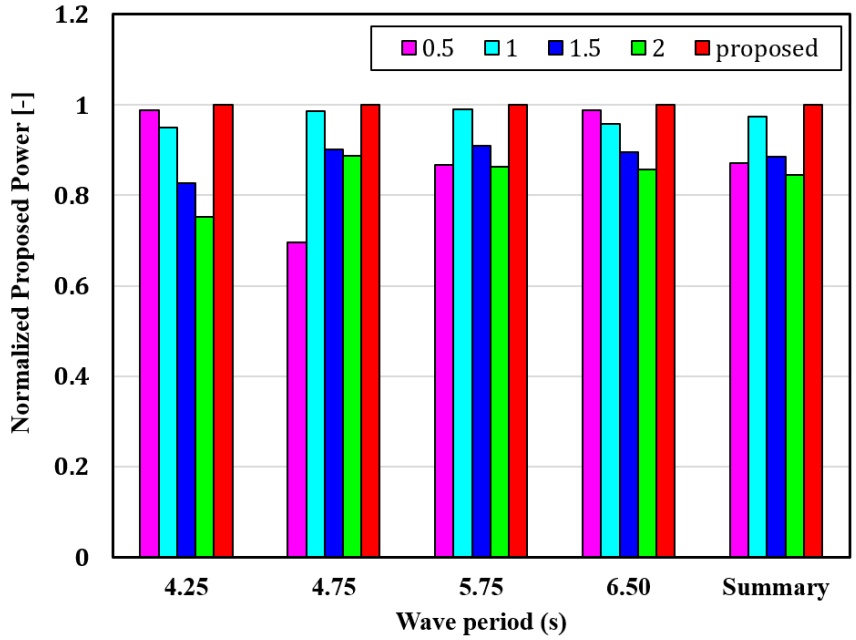

Figure 16. Comparison of power generation of conventional TCA with PTO damping coefficient change and proposed TCA.

5. Conclusions

The hydraulic system is mainly used for FWECs because it facilitates the control of low speed and high torque. A control algorithm to obtain maximum power is required because the wave energy converter has highly variable wave excitation moments; however, there are still only a few conventional studies on a control algorithm to obtain maximum power. Therefore, this paper proposes a control algorithm to obtain the maximum power by modeling a hydraulic system-based integrated wave energy converter. Although the power generation performance analysis was conducted based on the control variables of the conventional TCA, the output power generation for each control variable changed significantly depending upon the period of wave excitation moment. Therefore, this paper proposes a TCA that can obtain the maximum power regardless of the period of wave excitation moment. The proposed TCA continuously monitors the power generation output and changes the PTO damping coefficient in the direction that facilitates an increase in the

power generation output. The proposed TCA increased the output power generation by up to 18% compared to each PTO damping coefficient of the conventional TCA. In conclusion, the proposed method obtained higher power generation, regardless of the wave excitation moment period, as compared to the conventional TCA.

Author Contributions: K.-H.K. and J.-Y.P. managed the project; C.R., Y.-J.H. and J.-Y.P. performed the numerical simulation and analysis; C.R. drafted the paper; J.-Y.P., K.-H.K. and S.-H.S. edited the paper. All authors contributed to this study. All authors have read and agreed to the published version of the manuscript.

Funding: This research was supported by a grant from National R&D Project "Development of Wave Energy Converters Applicable to Breakwater and Connected Micro-Grid with Energy Storage System" funded by Ministry of Oceans and Fisheries, Korea (PMS4590). This research was supported by a grant from the Endowment Project of "Development of WECAN for the Establishment of Integrated Performance and Structural Safety Analytical Tools of Wave Energy Converter" funded by the Korea Research Institute of Ships and Ocean Engineering (PES3980). All support is gratefully acknowledged.

Institutional Review Board Statement: Not applicable.

Informed Consent Statement: Not applicable.

Data Availability Statement: Not applicable.

Conflicts of Interest: The authors declare no conflict of interest.

Abbreviations

The following abbreviations are used in this manuscript:

ω_{pitch}, θ_{pitch}	Angle and angular velocity of pitch motion
Q_{pump}	Flow rate of the pump
D_{pump}	Pump volume
F_{PTO}	Power take off force
P_H, P_L	High and low pressure in hydraulic circuit
Q_{check}, Q_{accu}, Q_{motor}	Flow rate in hydraulic circuit: check valve, accumulator, hydraulic motor
V_{accu}	Accumulator volume
P_{H_pre}	Initial pressure of the accumulator
V_{accu_pre}	Initial volume of the accumulator
T_m	Hydraulic motor torque
D_{motor}	Hydraulic motor volume
ω_{motor}	Angular speed of hydraulic motor
T_e	Electrical torque of generator
T_{fric}	Friction force of hydraulic motor
V_{mag}	back electromotive force of the generator
k_e	Back EMF constant of generator
P_e	Electrical power of the generator
J	Inertia of the hydraulic motor and generator
V_{sd} , V_{sq}	*d-q* voltage of generator
L_{sd}, L_{sq}	*d-q* inductance of generator
i_d, i_q	*d-q* current of generator
Ψ_{pm}	Generator flux linkage
ω_e	Electrical angular frequency
R_s	Phase resister of generator
N_p	Number of generator pole pair
ω_{wave}	Period of input wave energy
ω_{reson}	Resonance period of input wave energy
P_{abs}	Input absorption power
B_{pto}	Power take-off damping factor
k_{opt}	Torque damping factor

V_{dc} , I_{dc}	Output DC voltage, current
Δk	Torque damping coefficient change

References

1. Drew, B.; Plummer, A.R.; Sahinkaya, M.N. A Review of Wave Energy Converter Technology. *Proc. Inst. Mech. Eng. A* **2009**, *223*, 887–902. [CrossRef]
2. Cruz, J. *Ocean Wave Energy—Current Status and Future Perspectives*; Springer: Berlin, Germany, 2008; p. 434.
3. Falcao, A.F.O. Wave energy utilization: A review of the technologies. *Renew. Sustain. Energy Rev.* **2010**, *14*, 899–918. [CrossRef]
4. Salter, S.H.; Taylor, J.R.M.; Caldwell, N.J. Power Conversion Mechanisms for Wave Energy. *Proc. Inst. Mech. Eng. M* **2002**, *216*, 1–27. [CrossRef]
5. Hansen, R.; Kramer, M.; Vidal, E. Discrete Displacement Hydraulic Power Take-Off System for the Wavestar Wave Energy Converter. *Energies* **2013**, *6*, 4001–4044. [CrossRef]
6. Penalba, M.; Ringwood, J. A Review of Wave-to-Wire Models for Wave Energy Converters. *Energies* **2016**, *9*, 506. [CrossRef]
7. Apoorv, A.; Vishnu, M.L.; Anup, A.; Subhashish, B. Adaptive control of a hybrid energy storage system for wave energy conversion application. In Proceedings of the 2019 IEEE Energy Conversion Congress and Exposition (ECCE), Baltimore, MD, USA, 29 September–3 October 2019.
8. Wu, F.; Zhang, X.P.; Ju, P. Application of the battery energy storage in wave energy conversion system. In Proceedings of the 2009 International Conference on Sustainable Power Generation and Supply, Nanjing, China, 6–7 April 2009.
9. Xiang, Z.; Ossama, A.; Wayne, W. Power Take-Off and Energy Storage System Static Modeling and Sizing for Direct Drive Wave Energy Converter to Support Ocean Sensing Applications. *J. Mar. Sci. Eng.* **2020**, *8*, 513.
10. Mueller, M.; Baker, N. Direct Drive Wave Energy Converters. Available online: http://www.cder.dz/download/upec-1.pdf (accessed on 23 July 2013).
11. Polinder, H.; Mueller, M.; Scuotto, M.; Prado, M. Linear Generator Systems for Wave Energy Conversion. In Proceedings of the 7th European Wave and Tidal Energy Conference, Porto, Portugal, 11–14 September 2007.
12. DNV-Carbon Trust. *Guidelines on Design and Operation of Wave Energy Converters*; Technical Report; Det Norske Vertitas, The Carbon Trust: Bærum, Norway, 2005. Available online: http://www.carbontrust.com/ (accessed on 1 May 2005).
13. EMEC. *Guidelines for Design Basis of Marine Energy Conversion Systems*; Technical Report; European Marine Energy Centre Ltd. (EMEC): Stromness, UK, 2009. Available online: http://www.emec.org.uk/ (accessed on 1 January 2009).
14. Hansen, R.; Andersen, T.; Pedersen, H. Model Based Design of Efficient Power Take-Off Systems for Wave Energy Converters. In Proceedings of the 12th Scandinavian International Conference on Fluid Power (SICFP 2011), Tampere, Finland, 18–20 May 2011; Volume 2, pp. 35–49.
15. Falcao, A.F.O. Modeling and Control of Oscillating-Body Wave Energy Converters with Hydraulic Power Take-Off and Gas Accumulator. *Ocean Eng.* **2007**, *34*, 2021–2032. [CrossRef]
16. Babarit, A.; Guglielmi, M.; Clément, A.H. Declutching Control of a Wave Energy Converter. *Ocean Eng.* **2009**, *36*, 1015–1024. [CrossRef]
17. Hansen, R.; Andersen, T.; Pedersen, H. Comparison of Reactive and Non-Reactive Control Strategies for Wave Energy Converters with Non-Ideal Power Take-Off Systems. *Renew. Energy* **2013**, *6*, 31.
18. Skinner, N. Wave Energy Converter Device. European Patent EP2284386A2, 16 February 2011.
19. Linjama, M.; Vihtanen, H.P.; Sipola, A.; Vilenius, M. Secondary Controlled Multi-Chamber Hydraulic Cylinder. In Proceedings of the 11th Scandinavian International Conference on Fluid Power, Linköping, Sweden, 2–4 June 2009; p. SICFP09.
20. Henderson, R. Design, Simulation, and Testing of a Novel Hydraulic Power Take-Off System for the Pelamis Wave Energy Converter. *Renew. Energy* **2006**, *31*, 271–283. [CrossRef]
21. Yemm, R.; Pizer, D.; Retzler, C.; Henderson, R. Pelamis: Experience from Concept to Connection. *Philos. Trans. A Math. Phys. Eng. Sci.* **2012**, *370*, 365–380. [CrossRef] [PubMed]
22. Joseba, L.A.; Carlos, A.U.J.; Jose, E.A.F. Power Take-Off Device for Wave Energy Transformation. European Patent EP2466118A1, 20 June 2012.
23. Lasa, J.; Antolin, J.C.; Angulo, C.; Estensoro, P.; Santos, M.; Ricci, P. Design, Construction and Testing of a Hydraulic Power Take-Off for Wave Energy Converters. *Energies* **2012**, *5*, 2030–2052. [CrossRef]
24. Hansen, R.; Andersen, T.; Pedersen, H. Determining Required Valve Performance for Discrete Control of PTO Cylinders for Wave Energy. In Proceedings of the ASME Symposium on Fluid Power and Motion Control (FPMC 2012), Bath, UK, 12–14 September 2012; American Society of Mechanical Engineers: New York, NY, USA, 2012; pp. 565–578.
25. Roh, C.; Par, J.Y.; Ha, Y.J.; Cheon, H.J.; Kim, J.H.; Shin, S.H. Real Sea Test Results Analysis of Load Control Algorithm for Array Wave Energy Converter. In Proceedings of the Korean Society for Marine Environment & Energy, Busan, Korea, 7 November 2020; pp. 82–88.
26. Ratanak, S.; Sean, C.; Sam, K.; Asher, S.; Ted, K.A. *PTO-Sim: Development of a Power Take Off Modeling Tool for Ocean Wave Energy Conversion. IEEE Power & Energy Society General Meeting (IEEE-PES 2015)*; IEEE Publications: Denver, CO, USA, 2015.
27. Ratanaks, S.; Asher, S.; Ted, B.; Kelley, R.; Carlos, M. Development of PTO-SIM: A Power Performance Module for the Open-Source Wave Energy Converter Code WEC-SIM. In Proceedings of the ASME 2015 34th International Conference on Ocean, Offshore and Arctic Engineering, Canadian (OMAE2015), St. John's, NL, Canada, 31 May–5 June 2015.

28. Abdelsalam, A.K.; Massoud, A.M.; Ahmed, S.; Enjeti, P.N. High-Performance Adaptive Perturb and Observe MPPT Technique for Photovoltaic Based Microgrids. *IEEE Trans. Power Electron.* **2011**, *26*, 1010–1021. [CrossRef]
29. Aleix, M.A.; Aitor, J.G.; Eugen, R.; Izaskun, G. Control Strategies Applied to Wave Energy Converters: State of the Art. *Energies* **2019**, *12*, 3115.
30. Garcia-Rosa, P.B.; Kulia, G.; Ringwood, J.V.; Molinas, M. Real-Time Passive Control of Wave Energy Converters Using the Hilbert-Huang Transform. *IFAC-PapersOnLine* **2017**, *50*, 14705–14710. [CrossRef]
31. Nielsen, K.M.; Pedersen, T.S.; Andersen, P.; Ambühl, S. Optimizing Control of Wave Energy Converter with Losses and Fatigue in Power Take off. *IFAC-PapersOnLine* **2017**, *50*, 14680–14685. [CrossRef]
32. Jin, S.; Patton, R.J.; Guo, B. Enhancement of wave energy absorption efficiency via geometry and power take-off damping tuning. *Energy* **2019**, *169*, 819–832. [CrossRef]
33. Jiang, X.; Day, S.; Clelland, D. Hydrodynamic responses and power efficiency analyses of an oscillating wave surge converter under different simulated PTO strategies. *Ocean Eng.* **2018**, *170*, 286–297. [CrossRef]
34. Korde, U.A. Preliminary consideration of energy storage requirements for sub-optimal reactive control of axisymmetric wave energy devices. *Annu. Rev. Control* **2015**, *40*, 93–101. [CrossRef]
35. Budal, K.; Falnes, J. Optimum operation of wave power converter. *Mar. Sci. Commun.* **1977**, *3*, 133–150.
36. Wu, J.; Yao, Y.; Zhou, L.; Göteman, M. Real-time latching control strategies for the solo Duck wave energy converter in irregular waves. *Appl. Energy* **2018**, *222*, 717–728. [CrossRef]
37. Faedo, N.; Olaya, S.; Ringwood, J.V. Optimal control, MPC and MPC-like algorithms for wave energy systems: An overview. *IFAC J. Syst. Control* **2017**, *1*, 37–56. [CrossRef]
38. Ha, Y.J.; Park, J.Y.; Shin, S.H. Numerical Study of Non-Linear Dynamic Behavior of an Asymmetric Rotor for Wave Energy Converter in Regular Waves. *Processes* **2021**, *9*, 1477. [CrossRef]